Published in final edited form as:
ACS Chem Biol. 2013 June 21; 8(6): 1241–1252. doi:10.1021/cb300582s.

Synthesis and SAR of Lehualide B – A Marine-derived Natural Product with Potent Anti-Multiple Myeloma Activity

Valer Jeso[†], **Chunying Yang**[‡], **Michael D. Cameron**[#], **John L. Cleveland**[‡,*], and **Glenn C. Micalizio**[†,*]

[†]Departments of Chemistry, The Scripps Research Institute, Scripps Florida, Jupiter, Florida 33458

[‡]Cancer Biology, The Scripps Research Institute, Scripps Florida, Jupiter, Florida 33458

[#]Molecular Therapeutics, The Scripps Research Institute, Scripps Florida, Jupiter, Florida 33458

Abstract

We report a concise and convergent laboratory synthesis of the rare marine natural product lehualide B that has led to the discovery that: (1) this compound has low nanomolar activity against human multiple myeloma cells, and (2) the anti-cancer effects of lehualide B and its analogs are selective (*i.e.*, they are ~ two to three orders of magnitude less toxic to human breast cancer cells). Synthetic lehualide B is shown to be an effective inhibitor of complex I of the mitochondrial electron transport chain, with potency similar to that observed for the terrestrial natural products piericidin A1 and rotenone – an observation that led to the discovery that piericidin A1 is also selectively cytotoxic toward human multiple myeloma cells. Interestingly, synthetic derivatives of lehualide B that resemble verticipyrone (an established complex I inhibitor composed of a γ-pyrone and a simple mono-unsaturated hydrophobic chain) lack the potent anti-myeloma activity of the natural product. Finally, the synthesis and evaluation of a collection of lehualide-inspired analogs led to the elucidation of structure-activity relationships for this rare natural product that established important roles for the substituted γ-pyrone head group and the skipped polyene side chain.

Marine-derived natural products continue to provide an exciting collection of therapeutically valuable leads that, due to their usually low availability from natural sources, require chemical synthesis to drive efforts focused on evaluating their potential value as medicines.[1–3] The lehualides (Figure 1A) are a family of pyrone-containing natural products recently isolated from Hawaiian and Tongan marine sponges (*Plakortis* sp.) that were originally shown to possess modest anticancer properties against ovarian (IGROV-ET) and leukemia (K562) cell lines.[4,5] Notably, members of this class have disparate toxicity profiles that stem from subtle variations in pyrone substitution and the composition of their aliphatic tail. For example, lehualides A–D (**1**–**4**) show varying brine shrimp toxicity that suggests that the γ-pyrone motif imparts maximal toxicity.[4] Further, lehualides A (**1**) and C (**3**) do not display toxicity in ovarian or leukemia cell lines that are sensitive to lehualides B (**2**) and D (**4**) [**2**, GI_{50} = 830 nM (IGROV-ET); **4**, GI_{50} = 730 nM (IGROV-ET) or 230 nM (K562)]. In line with these observations that indicate a role for the γ-pyrone in imparting maximal toxicity, the most recently isolated lehualides (F–I; **6**–**9**) that contain α-pyrones similar to

Corresponding Authors: micalizio@scripps.edu; jcleve@scripps.edu.

Supporting information. Experimental procedures and tabulated spectroscopic data for new compounds (PDF) are available free of charge via the Internet at http://pubs.acs.org.

lehualide A (**1**) and monounsaturated or saturated hydrophobic side chains are much less toxic (1–2 orders of magnitude) than lehualides B and D.[5]

While the mechanism of action for the most toxic lehualides has heretofore not been elucidated, their common pyrone structure is reminiscent of the pyridine core of piericidin A1 and the quinone of ubiquinone (Figure 1B). Related γ-pyrone moieties are found in several other cytotoxic natural products (Figure 1C)[6–25] that have a wide variety of activities as insecticidal, anticancer, antifungal, antibacterial and immunosuppressive agents.[6–25] Some of these compounds have been shown to block the voltage-gated potassium channel Kv1.3 and to potently inhibit the mitochondrial electron transport chain protein NADH-ubiquinone reductase (complex I), with IC_{50}'s as low as 0.3 nM (verticipyrone analogs).[26] Finally, germane to our studies, a subset of potent complex I inhibitors have received attention as selective antitumor agents, yet the mechanism responsible for this activity has not been resolved.[27, 28]

Recent studies by Boger and colleagues focused on understanding the activity of piericidin A1 revealed that complex I inhibition is necessary but not sufficient to confer potent cytotoxicity to synthetic analogs. Hypotheses stated to explain this included a potential differential ability to access the cellular target, subtle distinctions between multiple binding sites on complex I, and/or a role for additional (undefined) biological targets.[28]

The most potent members of the lehualide family are structurally related to the natural products depicted in Figure 1B and 1C, yet they have unique features that include a 2,3-dimethoxy-substituted γ-pyrone and a hydrophobic tail that contains three trisubstituted alkenes that are uniformly "skipped" (non-conjugated) with respect to neighboring π-systems (*i.e.*, **2**). While not possessing a single chiral center, the stereochemistry and substitution of this skipped-polyunsaturated tail renders lehualide B a significant challenge to modern synthetic organic chemistry.[29]

The structural similarity of lehualide B to natural products known to possess an array of medicinally relevant biological activities, and the lack of a robust supply from natural sources prompted us to define a concise synthetic entry to this natural product that would allow assessment of the medicinal value of this target. In pursuit of these goals, our efforts have led to: (1) the total synthesis of lehualide B and twenty five synthetic analogs; (2) the discovery that lehualide B is selectively cytotoxic to multiple myeloma cells at low nanomolar concentrations; (3) the observation that lehualide B, and closely related synthetic analogs, totally abolish long-term growth of chemoresistant multiple myeloma cells; and (4) the discovery that lehualide B is a potent inhibitor of mitochondrial complex I.

RESULTS AND DISCUSSION

Total Synthesis of Lehualide B

Given anticipated difficulties associated with synthesizing the skipped polyene tail of **2**, our retrosynthetic strategy was primarily influenced by the most challenging structural motif in this region: the C12–C16 1,4-diene that houses both an (*E*)- and (*Z*)-trisubstituted alkene (Figure 2A). While modern carbonyl olefination or metal-catalyzed cross-coupling are commonly used for the synthesis of trisubstituted alkenes, neither of these is optimal for the challenge associated with this section of lehualide B. Specifically, methods based on carbonyl olefination are plagued by challenges associated with the control of stereochemistry in establishing the trisubstituted alkenes and with difficulties associated with advancing β, γ-unsaturated systems. [30] Metal-catalyzed cross-coupling is similarly complex owing to the multistep nature of synthetic pathways to generate the stereodefined coupling partners (Figure 2B) and to associated problems with regio- and stereocontrol in

the reaction of intermediate π-allyl complexes.[31] Given these hurdles we sought an alternative method for preparing this stereodefined subunit.

We recently established a reductive cross-coupling process that proceeds by stereoselective union of allylic alcohols with alkynes and that generates two stereodefined trisubstituted alkenes along with a central C–C bond.[32] In analyzing the lehualide B structure this reaction seemed ideal for establishing the C14–C15 bond with concomitant generation of each stereodefined trisubstituted alkene of the 1,4-diene – a bond construction that would ensue with stereo-undefined and 'unactivated' π-systems (Figure 2C).

Using this bond construction as a central feature of our design, the retrosynthetic strategy to lehualide B that emerged was comprised of a simple sequence that embraced the utility of allylic alcohols for establishing all of the trisubstituted alkenes in this target (Figure 2D). Well-established Claisen rearrangement chemistry[33, 34] was envisioned as a means to convert allylic alcohol **12** to an (*E*)-trisubstituted alkene (as in **11**), while Ti-mediated, alkoxide-directed reductive cross-coupling could then be employed to convert allylic alcohol **11** to the desired (*Z*)-trisubstituted C12-C13 alkene of lehualide B. In this latter process, stereochemical control was predicted in accord with our previous studies that put forth an empirical model based on a boat-like transition state geometry for carbometalation that features minimization of A1,2-strain (Figure 2C; **A** → **B** → **C**).[32]

With this retrosynthetic strategy in mind, we began with synthesis of the requisite 2,3-dimethoxy-5,6-dimethyl γ-pyrone **13**. As shown in Scheme 1A, iodosobenzene diacetate-mediated oxidation of β-ketoester **14** in methanol provided the α-methoxy-β-ketoester **15** in 70% yield.[35] Deprotonation with LDA (2.2 equiv), followed by addition of Weinreb amide **16**, then delivered the tricarbonyl **17** as a mixture of isomers. Stirring this tricarbonyl in neat H_2SO_4 (for 21 hr) then generated the γ-pyrone **13** in 24% yield over the two-step sequence.[36]

Next, attempted addition of the extended enolate of **13** to methacrolein was problematic, likely due to competitive 1,4-addition (Scheme 1B). To avoid this issue, α-(phenylseleno)-isobutyraldehyde was used as the electrophile in reaction with the anion of **13**. Subsequent oxidation to the selenoxide was followed by *syn*-elimination *in situ* to deliver the desired allylic alcohol **12** in 73% yield (over two steps).[37] Next, Johnson orthoester Claisen rearrangement delivered the desired γ,δ-unsaturated aldehyde (*E*:*Z* = 10:1),[38] which was then used to generate the functionalized allylic alcohol **11** by the addition of 2-propenylmagnesium bromide (53% yield over two steps).

Having the allylic alcohol **11** in hand, alkoxide-directed Ti-mediated reductive cross-coupling with 1-phenyl-2-butyne was then performed using slightly modified reaction conditions than previously reported for this stereoselective coupling process.[32] Initial formation of a dianion of **11** (to mask the potential electrophilic character of the pyrone carbonyl) was followed by exposure to a preformed Ti–alkyne complex that was generated by treating 1-phenyl-2-butyne with a combination of $ClTi(O\textit{i}\text{-}Pr)_3$ (6 equiv) and *c*-C_5H_9MgCl (12 equiv). Warming from −78 to 0 °C, followed by an aqueous quench, delivered the coupled products in 50% combined yield.

Despite the success of this coupling process and the concise synthetic sequence (six steps from the simple γ-pyrone), the natural product was formed as an inseparable 1.3:1 mixture of regioisomers (**2** and **19**), where the minor product was derived from C–C bond formation occurring α-to the Bn substituent of the alkyne to deliver iso-lehualide B. This low selectivity was expected, as regiochemical control in functionalizing Ti–alkyne complexes typically requires substantial steric or electronic differentiation of the alkyne termini.[39] In

the competing transition states for carbometalation depicted in Scheme 1C, it is evident that the steric impediment of the Ph group can easily be avoided by simple bond rotation (this similar steric profile of Me and Bn is evident in their A values: Me = 1.7 kcal/mol; Bn = 1.8 kcal/mol[40]).

To circumvent this problem, a straightforward solution was adopted that exploited the well-appreciated regioselectivity associated with Ti-mediated reductive cross-coupling reactions of TMS-substituted alkynes.[39] Specifically, metallacycle-mediated reductive cross-coupling of allylic alcohol **11** with TMS-propyne (**20**, Scheme 1D) delivered the TMS-alkene-containing 1,4-diene product **21** in 61% yield (*Z:E* = 7:1; rs ≥20:1). Subsequent conversion to the vinyliodide [NIS, $ClCH_2CN$:EtOAc (2:1)],[41] followed by Pd-catalyzed cross-coupling with benzylzinc bromide generated lehualide B in 64% yield over the final two-step sequence.[42]

Anti-Cancer Properties of Lehualide B

The concise synthesis of lehualide B fueled efforts to prepare sufficient quantities of the natural product to evaluate its anti-cancer properties. Our initial assessment of the effects of 0.1–10μM doses of lehualide B on a cast of tumor cell lines was performed with MTT assays using estrogen receptor-positive (ER+) (MCF7, T47D) and triple negative (MDA-MB-231, HS578) breast cancer cells, and three multiple myeloma (MM) cell lines (NCI H929, U266, and RPMI-8266).[43] While there were essentially no effects of lehualide B on the growth of triple-negative breast cancer, and only modest effects on ER+ breast cancer cells, there were profound effects on multiple myeloma cells (Figure 3A). Indeed, MTT assays established very potent activity for lehualide B in all MM tumor cell lines investigated, with EC_{50} values of 2.1, 2.9, and 13 nM for RPMI-8226, U266 and NCI H929 MM cells, respectively. Interestingly, lehualide B was three orders of magnitude less effective *vs.* MCF7 and T47D ER+ breast cancer cells (> 1μM, Figure 3) and > 1 order of magnitude less toxic to mouse bone marrow-derived primary B cells cultured on stroma and in IL7 medium (EC_{50} of 92 nM, Figure 3B). Thus, there is significant selectivity associated with the cytotoxic profile of lehualide B.

To address the mechanism by which lehualide B compromised MM cells, its effects were assessed on cell growth using standard growth assays and upon cell survival by trypan blue dye exclusion.[44] Human MM cells and Raji B lymphoma were plated in culture and then treated with lehualide B for two days. Notably, treatment with the natural product led to rapid and marked reductions in cell number that were accompanied by a loss in cell viability (Figure 3C) and cell shrinkage (especially in NCI H929 MM) typical of apoptotic cell death.

Given the structural similarity of the γ-pyrone group of lehualide B with the quinone of ubiquinone and the hetero-cycle of piericidin A1, we tested if lehualide B was an inhibitor of complex I of the mitochondrial electron transport chain. Indeed, in vitro assays established that, like piericidin A1, lehualide B is a potent complex I inhibitor (IC_{50} = 30 nM; Figure 3D).

These findings suggested that other complex I inhibitors may display similar anti-myeloma activity. Indeed, piericidin A1 and rotenone also block the proliferation of U266 and RPMI-8226 MM cells (Figure 3E and data not shown). Related to the profile of lehualide B, these agents were similarly ineffective *vs.* breast cancer cells (data not shown). Thus, mitochondrial complex I inhibitors such as lehualide B and piericidin A1 are selective anti-cancer agents and have high potency against multiple myeloma. In addition to discovering this interesting anticancer activity of lehualide B, to our knowledge this is the first report that describes the potent and selective anti-MM properties associated with piericidin A1.

To assess why MM cells are so sensitive to complex I inhibitors such as lehualide B while others such MDA-MB-231 breast cancer cells are not, we evaluated the metabolic status of these tumor cells and how this is affected by treatment with lehualide B using the Seahorse Bioscience XF96 Analyzer.[45] Specifically, we assessed the effects of lehualide B on the oxygen consumption rate (OCR, a measure of oxidative phosphorylation [OXPHOS]) and extracellular acidification rate (ECAR, a measure of aerobic glycolysis). Notably, these analyses demonstrated that U266 MM cells have much higher rates of OCR than MDA-MB-231 breast cancer cells and that lehualide B treatment abolishes OCR and depletes mitochondrial energy reserves, as demonstrated by treatment of cells with the mitochondrial uncoupling agent FCCP (Figure 4). Furthermore, lehualide B causes a marked shift in metabolism to ECAR (Figure 4B–C). We conclude that U266 MM cells rely on OXPHOS (OCR) to support their metabolism, which is disabled by lehualide B, whereas the metabolism of MDA-MB-231 breast cancer cells rather relies on aerobic glycolysis.

Synthesis and Activity of Lehualide B Analogs

The potent and selective anti-MM profile of lehualide B, and the lack of substantive structure-activity relationships for this rare marine-derived natural product, prompted analyses of the molecular features essential for its anti-myeloma activity. We investigated the role that three key regions of the natural product play in imparting anti-MM properties: (1) the aromatic tail, (2) the hydrophobic linker, and (3) the γ-pyrone hydrophilic head group.

Series I analogs were prepared to evaluate the significance of the entire hydrophobic tail of lehualide B (including the aromatic terminus). These analogs were generated as described in Figure 5A, and follow either: (1) nucleophilic addition of a pyrone-derived anion to an allylic halide (eq 1); (2) nucleophilic addition of a pyrone-derived anion to an aldehyde (eq 2); or (3) nucleophilic addition to a pyrone-containing unsaturated aldehyde (eq 3). Analogs were prepared with prenyl, geranyl and farnesyl side chains (**22**–**24**), as well as varying saturated/unsaturated motifs (**25**–**27** and **11**). Notably, while all of these analogs retained the substituted γ-pyrone of lehualide B, none of them showed significant anti-myeloma activity (all had EC_{50} values > 1μM in U266 MM cells; Figure 5B), indicating a significant role for the stereodefined skipped polyene subunit of the natural product.

Series II analogs assessed the effect of alterations to the tail of the hydrophobic linker (Figure 5C), while maintaining the functionalized 2,3-dimethoxy-5,6-dimethyl-γ-pyrone core and the hydrophobic polyunsaturated linker. Analogs were prepared from the general sequence shown in Figure 5C, defined by Grignard addition to an unsaturated pyrone-containing aldehyde, followed by Ti-mediated alkoxide-directed reductive cross-coupling. While derivatives **28**–**30**, showed substantially diminished anti-MM activity (EC_{50}'s of 100–600 nM), a variety of other substitutions were tolerated in this region. The most active analogs prepared include the C15- and C16-biphenyls (**31** and **35**; EC_{50}'s of 10–12 nM), and the C12-Et substituted variant **36** (EC_{50} = 13 nM)(Figure 5D). Other analogs possessing notable activity include the C14-Ph (**32**; EC_{50} 60 nM), the C-15 protio (**33**; EC_{50} 30 nM), the C15-TMS (**21**; EC_{50} 20 nM) and the C15 chloropentyl derivative (**34**; EC_{50} 60 nM).

Finally, Series III analogs were synthesized to determine the effects of subtle structural perturbations about the pyrone head-group (Figure 6A). The synthesis of each analog within this series was accomplished in a fashion akin to that described for lehualide B synthesis (Scheme 1D), where the variation in structure of the pyrone was introduced at the beginning of each sequence.

As illustrated, deletion of the 2,3-dimethoxy substituent of lehualide B essentially abolished anti-myeloma activity, where compounds **37** and **38** displayed markedly reduced abilities to

inhibit the growth of U266 MM cells (EC_{50} > 1μM). Notably, substitution α- to the pyrone also obliterated the cytotoxic properties of lehualide B. For example, analog **41** that houses a prenyl substituent at this position did not inhibit MM or lymphoma cell growth at concentrations greater than 1μM. The most potent Series III analogs were those that simply replaced the C3 methyl ether of the pyrone with an ethyl group. Analogs **42**–**44** were the most active members of this series, with EC_{50} values *vs.* U266 MM cells of 19, 3 and 20 nM, respectively.

Anti-Myeloma Effects of Lehualide B Analogs

The effects of lehualide B and top analogs showing anti-myeloma and lymphoma activity in MTT assays suggested that they would also compromise the long-term, anchorage-independent growth of MM in methylcellulose colony assays.[46] Indeed, treatment with lehualide B, **36**, **42**, or **43** completely abolished colony formation of NCI H929 and U266 MM cells (Figure 6B–D), further supporting their potential use as anti-myeloma agents.

Over 70,000 patients in the United States currently suffer from multiple myeloma (MM), with 20,000 new cases and 10,000 deaths per year.[47] Morbidity associated with this malignancy is very high, with patients experiencing anemia, chronic bone pain and fractures, and an overall 5-year survival still below 40% despite aggressive chemotherapy, up-front bone marrow transplantation, the novel use of agents such as thalidomide, and the development of new drugs such as bortezomib.

The marine-derived natural product lehualide B was originally reported to have modest activity against IGROV-ET ovarian cancer cells.[4] While no other biological properties had been assigned to this compound, its modest activity, unique chemical structure, and lack of availability from natural sources stimulated our interest in exploring a means to prepare this compound (and related derivatives) in the laboratory to fuel efforts focused on thoroughly evaluating its efficacy as an anticancer agent.

Notably, we achieved a concise synthesis of this target in just eight steps from a simple γ-pyrone through a sequence that highlights the unique and divergent stereochemical course of allylic alcohol–alkyne reductive cross-coupling when compared to the Claisen rearrangement. Both processes were used back-to-back to establish the entire stereodefined hydrophobic tail of lehualide B, and generated each of the three trisubstituted alkenes with just four carbon–carbon bond forming reactions (Claisen rearrangement, Grignard addition, Ti-mediated reductive cross-coupling and Negishi coupling).

The concise nature of this synthesis fueled our pursuits that have defined the substantial anti-multiple myeloma properties of lehualide B. In short order it was discovered that lehualide B possesses rather profound and selective anti-multiple myeloma activity, having low nanomolar EC_{50} activity in human MM and Raji B lymphoma, and low or no activity against human breast cancer.

Our studies established that lehualide B has similar activity to piericidin A1 as a potent inhibitor of complex I. Establishing this relationship led to the discovery that piericidin A1 also has selective activity against MM. These findings add to the interesting anti-cancer profile of piericidin A1 that, to date, includes toxicity against human NSCLC, leukemia and colon carcinoma. [28, 48–50] We conclude that at least some mitochondrial complex I inhibitors, specifically lehualide B and piericidin A1, are selective anti-cancer agents that have profound cytotoxic activity against chemoresistant multiple myeloma cells. Further, our studies suggest that tumor types that rely on OXPHOS to support their metabolism, such as MM, will be exquisitely sensitive to complex I inhibitors such as lehualide B. Finally, the sensitivity of MM cells to complex I inhibitors may also reflect the massive production of

immunoglobulins and inherently high activity of the endoplasmic reticulum (ER) in this tumor type.[51] Specifically, mitochondria function to balance Ca^{2+} pools in the lumen of ER and their inhibition would lead to Ca^{2+} loss and cell death.

Our *in vivo* evaluations of lehualide B revealed that dosing *i.p.* (1mg/kg) in sub-Q transplant models of RPMI 8226 and U266 MM cells led to tumor drug concentrations that were an order of magnitude higher than the EC_{50} value of lehualide B in cellular assays. While promising, much higher concentrations were, however, found in fat, kidney and heart. The relevance of tissue distribution data are difficult to extrapolate across species, yet these findings indicate that the DMPK profile for lehualide B (and perhaps its analogs) needs substantial improvement or that a targeted drug delivery strategy needs to be established before advancing as a clinically relevant anti-myeloma agent.

The compelling anti-multiple myeloma profile of lehualide B prompted the investigation of structure–activity relationships associated with the natural product. Over twenty analogs were prepared to evaluate the role of three regions of the natural product skeleton (the hydrophobic tail terminus, the hydrophobic polyunsaturated linker, and the hydrophilic head-group) in anticancer activity. These studies led to the general summary of SAR illustrated in Figure 7 and include the following features:

1. The stereodefined skipped-polyunsaturated hydrophobic tail plays a critical role in cytotoxicity. This observation is similar to that observed with piericidin analogs, where simplified hydrophobic chains appended to the pyridine core compromise cytotoxicity.[28] Similar trends have also been observed with verticipyrone.[52]
2. The terminal substituents of the hydrophobic chain of lehualide B play an important role in anti-MM activity. Small substituents are optimal at C15, while some modifications of C16 functionality are tolerated (small alkyl and aryl).
3. Anti-MM activity is sensitive to the substitution of the pyrone head-group. The only synthetic analogs that possess similar activity to the natural product had a simple change of substitution at C3 of the pyrone from OMe to Et. All other attempted modifications to this region of the natural product markedly reduced anti-MM activity.

Overall, these studies have established a chemical foundation suitable for the production of lehualide-inspired agents. This achievement led to the elucidation of lehualide B's activity as a complex I inhibitor and the discovery that this natural product possesses profound anti-multiple myeloma properties. While the development of lehualide B as a chemotherapeutic agent is anticipated to be challenging, the chemical advance central to these studies provides a means to drive the search for therapeutically relevant natural product analogs.

Supplementary Material

Refer to Web version on PubMed Central for supplementary material.

Acknowledgments

We gratefully acknowledge financial support of this work by grants from the National Institutes of Health/NIGMS (GM80266, GM80266-04S1, to G. C. Micalizio) and NCI (CA076379, to J. L. Cleveland), and by monies from the State of Florida to Scripps Florida.

References

1. Morris E. Marine natural products: Drugs from the deep. Nature. 2006; 443:904–905. [PubMed: 17066005]

2. Miller JH, Singh AJ, Northcote PT. Microtubule-stabilizing drugs from marine sponges: focus on peloruside A and zampanolide. Marine Drugs. 2000; 8:1059–1079. [PubMed: 20479967]
3. Simmons TL, Andrianasolo E, McPhail K, Flatt P, Gerwick WH. Marine natural products as anticancer drugs. Mol Cancer Ther. 2005; 4:333–342. [PubMed: 15713904]
4. Sata N, Abinsay H, Yoshida WY, Horgen FD, Sitachitta N, Kelly M, Scheuer PJ. Lehualides A–D, metabolites from a Hawaiian sponge of the genus *Plakortis*. J Nat Prod. 2005; 68:1400–1403. [PubMed: 16180823]
5. Barber JM, Quek NCH, Leahy DC, Miller JH, Bellows DS, Northcote PT. Lehualides E-K, cytotoxic metabolites from the Tongan marine sponge Plakortis sp. J Nat Prod. 2011; 74:809–815. [PubMed: 21351759]
6. Wilk W, Waldmann H, Kaiser M. Gamma-pyrone natural products--a privileged compound class provided by nature. Bioorg Med Chem. 2009; 17:2304–2309. [PubMed: 19042133]
7. Wetzel S, Wilk W, Chammaa S, Sperl B, Roth AG, Yektaoglu A, Renner S, Berg T, Arenz C, Giannis A, Oprea TI, Rauh D, Kaiser M, Waldmann H. A scaffold-tree-merging strategy for prospective bioactivity annotation of gamma-pyrones. Angew Chem Int Ed. 2010; 49:3666–3670.
8. Foucher B, Chappell JB, McGivan JD. The effects of acetylcolletotrichin on the mitochondrial respiratory chain. Biochem J. 1974; 138:415–423. [PubMed: 4372992]
9. Singh SB, Zink DL, Dombrowski AW, Dezeny G, Bills GF, Felix JP, Slaughter RS, Goetz MA. Candelalides A–C: Novel diterpenoid pyrones from fermentations of *Sesquicillium candelabrum* as blockers of the voltage-gated potassium channel Kv1.3. Org Lett. 2001; 3:247–250. [PubMed: 11430046]
10. Goetz MA, Zink DL, Dezeny G, Dombrowski A, Polishook JD, Felix JP, Slaughter RS, Singh SB. Diterpenoid pyrones, novel blockers of the voltage-gated potassium channel Kv1.3 from fungal fermentations. Tetrahedron Lett. 2001; 42:1255–1257.
11. Bills GF, Polishook JD, Goetz MA, Sullivan RF, White JF Jr. *Chaunopycnis pustulata* sp. nov., a new clavicipitalean anamorph producing metabolites that modulate potassium ion channels. Mycol Prog. 2002; 1:3–17.
12. Gupta S, Krasnoff SB, Renwick JAA, Roberts DW, Steiner JR, Clardy J. Viridoxins A and B: novel toxins from the fungus *Metarhizium flavoviride*. J Org Chem. 1993; 58:1062–1067.
13. Ui H, Shiomi K, Suzuki H, Hatano H, Morimoto H, Yamaguchi Y, Masuma R, Sunazuka T, Shimamura H, Sakamoto K, Kita K, Miyoshi H, Tomoda H, Omura S. Verticipyrone, a new NADH-fumarate reductase inhibitor, produced by *Verticillium* sp. FKI-1083. J Antibiot. 2006; 59:785–790. [PubMed: 17323645]
14. Kurosawa K, Takahashi K, Fujise N, Yamashita Y, Washida N, Tsuda E. SNF4435C and D, novel immunosuppressants produced by a strain of Streptomyces spectabilis. III Immunosuppressive efficacy. J Antibiot. 2002; 55:71–77. [PubMed: 11918069]
15. Ueda J, Hashimoto J, Nagai A, Nakashima T, Komaki H, Anzai K, Harayama S, Doi T, Takahashi T, Nagasawa K, Natsume T, Takagi M, Shin-ya K. New aureothin derivative, alloaureothin, from *Streptomyces* sp. MM23. J Antibiot. 2007; 60:321–324. [PubMed: 17551211]
16. Kurosawa K, Takahashi K, Tsuda E. SNF4435C and D, novel immunosuppressants produced by a strain of *Streptomyces spectabilir I Taxanomy, fermentation, isolation, and biological activities*. J Antibiot. 2001; 54:541–547. [PubMed: 11560371]
17. Takahashi K, Tsuda E, Kurosawa K. SNF4435C and D, novel immunosuppressants produced by a strain of Streptomyces spectabilis - II. Structure elucidation. J Antibiot. 2001; 54:548–553. [PubMed: 11560372]
18. Yano K, Yokoi K, Sato J, Oono J, Kouda T, Ogawa Y, Nakashima T. Actinopyrones A, B and C, new physiologically active substances. II Physico-chemical properties and chemical structures. J Antibiot. 1986; 39:38–43. [PubMed: 3753970]
19. Yano K, Yokoi K, Sato J, Oono J, Kouda T, Ogawa Y, Nakashima T. Actinopyrones A, B and C, new physiologically active substances. J Antibiot. 1986; 39:32–37. [PubMed: 3753969]
20. Taniguchi M, Watanabe M, Nagai J, Suzumura K-I, Suzuki K-I, Tanaka A. γ-Pyrone compounds with selective and potent anti-*Helicobacter pylori* activity. J Antibiot. 2000; 53:844–847. [PubMed: 11079808]

21. Graber MA, Gerwick WH. Kalkipyrone, a toxic γ-pyrone from an assemblage of the marine cyanobacteria *Lyngbya majuscula* and *Tolypothrix* sp. J Nat Prod. 1998; 61:677–680. [PubMed: 9599278]
22. Yoshida S, Yoneyama K, Shiraishi S, Watanabe A, Takahashi N. Isolation and physical properties of new piericidins produced by *Streptomyces pactum*. Agric Biol Chem. 1977; 41:849–853.
23. Yoshida S, Yoneyama K, Shiraishi S, Watanabe A, Takahashi N. Chemical structures of new piericidins produced by *Streptomyces pactum*. Agric Biol Chem. 1977; 41:855–862.
24. Kimura K, Takahashi H, Miyata N, Yoshihama M, Uramoto M. New piericidin antibiotics, 7-demethylpiericidin A1 and 7-demethyl-3′-rhamnopiericidin A1. J Antibiot. 1996; 49:697–699. [PubMed: 8784434]
25. For the combinatorial synthesis and evaluation of a collection of benzopyran natural product-like inhibitors of NADH:ubiquinone oxidoreductase, see: Nicolaou KC, Pfefferkorn JA, Schuler F, Roecker AJ, Cao GQ, Casida JE. Combinatorial synthesis of novel and potent inhibitors of NADH:ubiquinone oxidoreductase. Chem Biol. 2000; 7:979–992. [PubMed: 11137820]
26. Shimamur H, Sunazuka T, Izuhara T, Hirose T, Shiomi K, Omura S. Total Synthesis and Biological Evaluation of Verticipyrone and Analogues. Org Lett. 2007; 9:65–67. [PubMed: 17192086]
27. Udeani GO, Geräser C, Thomas CF, Moon RC, Kosmeder JW, Kinghorn AD, Moriarty RM, Pezzuto JM. Cancer chemopreventive activity mediated by deguelin, a naturally occurring rotenoid. Cancer Res. 1997; 57:3424–3428. and references therein. [PubMed: 9270008]
28. Schnermann MJ, Romero FA, Hwang I, Nakamaru-Ogiso E, Yagi T, Boger DL. Total synthesis of piericidin A1 and B1 and key analogues. J Am Chem Soc. 2006; 128:11799–11807. [PubMed: 16953619]
29. Jeso V, Micalizio GC. Total synthesis of lehualide B by allylic alcohol–alkyne reductive cross-coupling. J Am Chem Soc. 2010; 132:11422–11424. [PubMed: 20681603]
30. For a recent example that highlights the sensitivity of β, γ-unsaturated carbonyls, see Gagnepain J, Moulin E, Füstner A. Gram-scale synthesis of Iejimalide B. Chem Eur J. 2011; 17:6964–6972. [PubMed: 21557354]
31. For a review of palladium-catalyzed cross-coupling reactions in total synthesis see Nicolaou KC, Bulger PG, Sarlah D. Palladium-catalyzed cross-coupling reactions in total synthesis. Angew Chem Int Ed. 2005; 44:4442–4489.
32. Kolundzic F, Micalizio GC. Synthesis of substituted 1,4-dienes by direct alkylation of allylic alcohols. J Am Chem Soc. 2007; 129:15112–15113. [PubMed: 18004854]
33. Rhoads SJ, Raulins R. Claisen and Cope rearrangements. Org React. 1975; 22:1–74.
34. Ziegler FE. The thermal, aliphatic Claisen rearrangement. Chem Rev. 1988; 88:1423–1452.
35. The procedure employed is a variation of that reported: Moriarty RM, Vaid RK, Ravikumar VT, Vaid BK, Hopkins TE. Hypervalent iodine oxidation: α-Functionalization of β-dicarbonyl compounds using iodosobenzene. Tetrahedron. 1988; 44:1603–1607.
36. For an early example of pyrone formation conducted in sulfuric acid (conc.) see: Light RJ, Hauser CR. Aroylations of β-diketones at the terminal methyl group to form 1,3,5-triketones. J Org Chem. 1960; 25:538–546.
37. Jones DN, Mundy D, Whitehouse RD. Steroidal selenoxides diastereoisomeric at selenium; *syn*-elimination, absolute configuration, and optical rotatory dispersion characteristics. Chem Commun. 1970:86–87.
38. For an early example see: Johnson WS, Werthem AL, Bartlett WR, Brocksom TJ, Li TT, Faulkner DJ, Petersen MR. Simple stereoselective version of the Claisen rearrangement leading to *trans*-trisubstituted olefinic bonds. Synthesis of squalene. J Am Chem Soc. 1970; 92:741–743.
39. Reichard HA, McLaughlin M, Chen MZ, Micalizio GC. Regioselective reductive cross-coupling reactions of unsymmetrical alkynes. Eur J Org Chem. 2010:391–409.
40. Anderson JE. Conformational analysis of cyclohexane derivatives. The *A* value of a benzyl group. J Chem Soc, Perkin Trans. 1974; 2:10–13.
41. Stamos DP, Taylor AG, Kishi Y. A mild preparation of vinyliodides from vinylsilanes. Tetrahedron Lett. 1996; 37:8647–8650.

42. For a recent review see: Jana R, Pathak TP, Sigman MS. Advances in transition metal (Pd,Ni,Fe)-catalyzed cross-coupling reactions using alkyl-organometallics as reaction partners. Chem Rev. 2011; 111:1417–1492. [PubMed: 21319862]
43. The MTT assay is a colorimetric assay for measuring the activity of enzymes that reduce 3-(4, 5-dimethylthiazol-2-yl)-2, 5-diphenyltetrazolium bromide (MTT). This reduction takes place only when reductase enzymes are active, and therefore conversion is often used as a measure of viable (living) cells. See: Mosmann T. Rapid colorimetric assay for cellular growth and survival: application to proliferation and cytotoxicity assays. J Immunol Methods. 1983; 65:55–63. [PubMed: 6606682]
44. The dye exclusion test is used to determine the number of viable cells present in a cell suspension. It is based on the principle that live cells possess intact cell membranes that exclude certain dyes, such a trypan blue, Eosin, or propidium, whereas dead cells do not. Overall, dye exclusion is a simple and rapid technique to measure cell viability indirectly via assessment of cell membrane integrity. See: Strober W. Trypan blue test of cell viability. Current Protocols in Immunology. 1997:A.3B.1–A.3B.2.
45. Wu M, Neilson A, Swift AL, Moran R, Tamagnine J, Parslow D, Armistead S, Lemire K, Orrell J, Teich J, et al. Multiparameter metabolic analysis reveals a close link between attenuated mitochondrial bioenergetic function and enhanced glycolysis dependency in human tumor cells. Am J Physiol Cell Physiol. 2007; 292:C125–136. [PubMed: 16971499]
46. Li Y, Li Ching J, Yu D, Pardee AB. Potent induction of apoptosis by beta-lapachone in human multiple myeloma cell lines and patient cells. Mol Med. 2000; 6:1008–1015. MTT assays assess the short-term anti-proliferative effects of anti-cancer agents, whilst methylcellulose colony assays are a more rigorous measure of the effects of such agents on long-term, anchorage-independent growth of tumor cells in semi-solid medium. [PubMed: 11474117]
47. Mahindra A, Laubach J, Raje N, Munshi N, Richardson PG, Anderson K. Latest advances and current challenges in the treatment of multiple myeloma. Nat Rev Clin Oncol. 2012; 9:135–143. [PubMed: 22349016]
48. Urakwa A, Sasaki T, Yoshida K, Otani T, Lei Y, Yun W. IT-143-A and B, novel piericidin-group antibiotics produced by *Streptomyces sp.* J Antibiotics. 1996; 49:1052–1055. [PubMed: 8968401]
49. Hwang J, Kim J, Cha M, Ryoo I, Choo S, Cho S, Tsukumo Y, Tomida A, Shin K, Hwang Y, Yoo I, Park H. Etoposide-resistant HT-29 human colon carcinoma cells during glucose deprivation are sensitive to piericidin A, a GRP78 down-regulator. J Cell Physiol. 2008; 215:243–250. [PubMed: 17941090]
50. Kitaura N, Shirata K, Niwano M, Mimura M, Takahara Y. Tumor cell inhibitors containing piericidin A, Japanese Patent 05339156 A2, (1994). Chem Abstr. 1993; 120:208590.
51. Kurtoglu M, Philips K, Liu H, Boise LH, Lampidis TJ. High endoplasmic reticulum activity renders multiple myeloma cells hypersensitive to mitochondrial inhibitors. Cancer Chemother Pharmacol. 2010; 66:129–140. [PubMed: 19779717]
52. Leiris SJ, Khdour OM, Segerman ZJ, Tsosie KS, Chapuis JC, Hecht SM. Synthesis and evaluation of verticipyrone analogues as mitochondrial complex I inhibitors. Bioorg Med Chem. 2010; 18:3481–3493. [PubMed: 20456960]

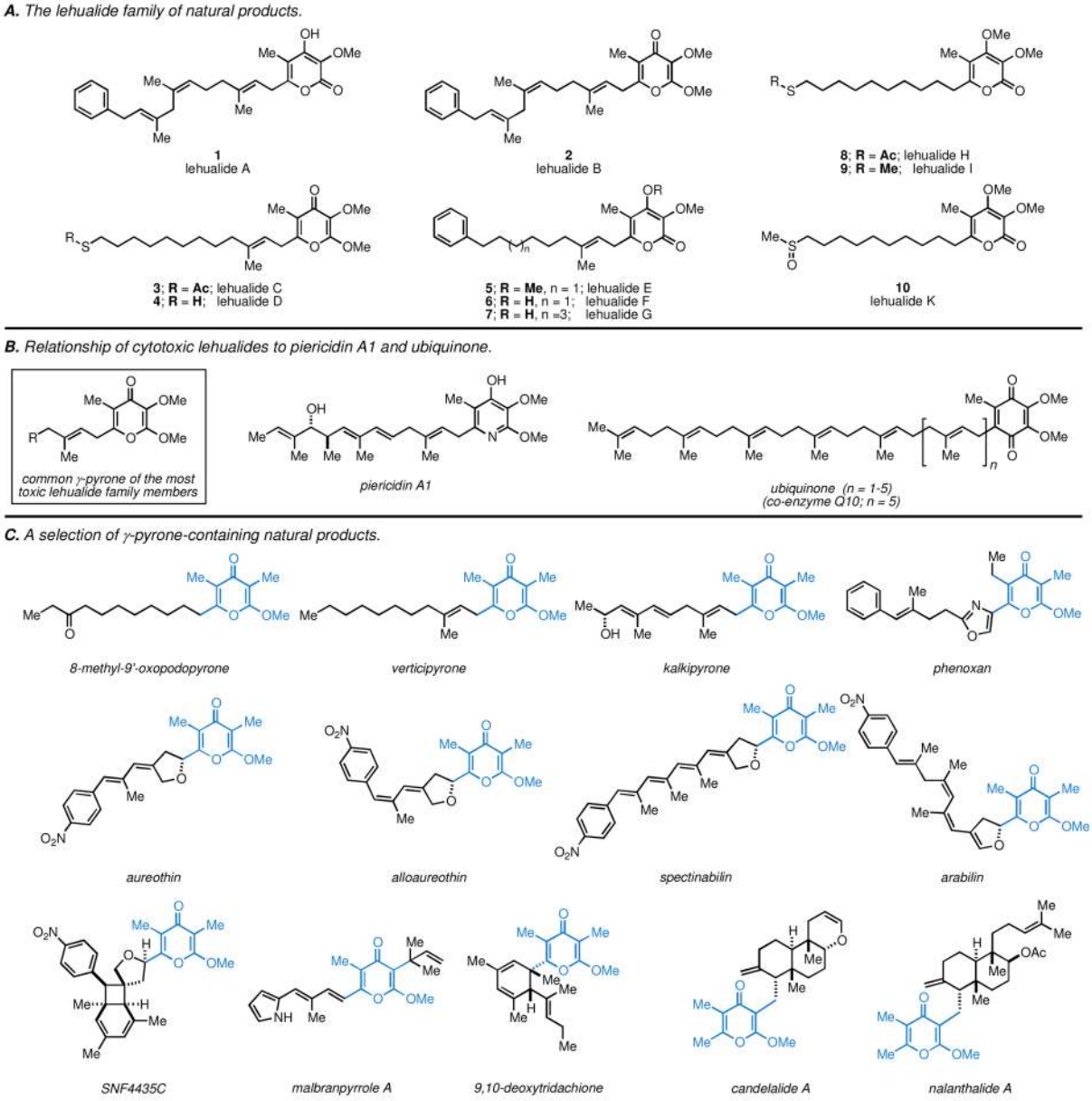

Figure 1.
Introduction to the lehualides and related natural products.

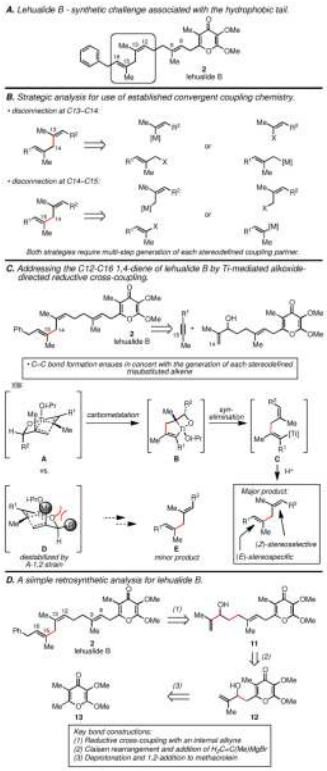

Figure 2.
Development of a concise synthesis strategy for lehualide B.

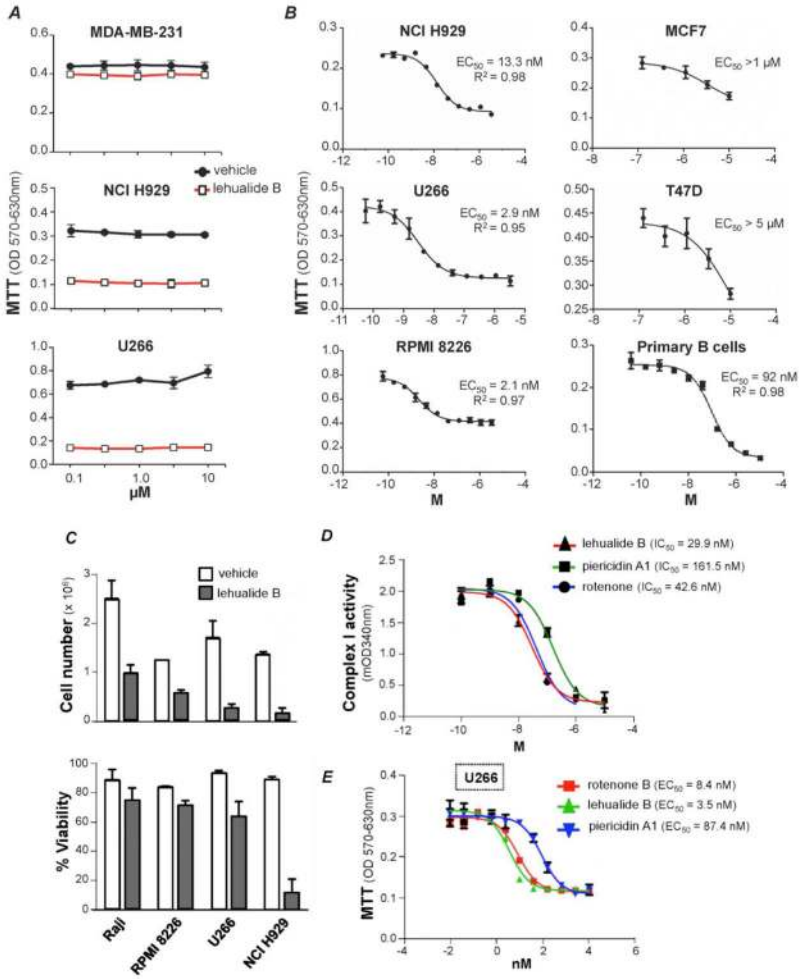

Figure 3.

Lehualide B has potent and selective activity against multiple myeloma (MM) cells, impairs MM cell growth and survival, and is a potent inhibitor of complex I of the mitochondrial electron transport chain. (***A***). MTT assays were performed on MDA-MB-231 triple-negative breast cancer cells and on NCI H929 and U266 MM cells, which were treated with the indicated doses of lehualide B (3 days of culture). (***B***) The EC_{50} values of lehualide B for the indicated MM cells (*left*) and bone marrow-derived primary mouse B cells were determined using 11-point dose-response MTT assays. For the ER+ breast cancer cells MCF7 and T47 D (*right*) the EC_{50} was > 1 μM (five-point dose-response MTT assays). Error bars are the SD of the mean (n =3). (***C***) The indicated tumor cell lines were incubated with 1 μM lehualide B or vehicle. Cell numbers (*top*) and viability (*bottom*) were determined after 4 days +/− lehualide B (30 nM). Error bars are the SD of the mean (n = 2). (***D***) Lehualide B blocks complex I. Mitochondrial complex I activity was measured using the MitoTox™ Complex I OXPHOS Activity assay kit. Error bars are the SD of the mean (n = 4) (***E***) Mitochondrial complex I inhibitors have potent anti-MM activity. U266 MM cells were treated with the indicated doses of lehualide B, piericidin A1, or rotenone for 3 days and MTT assays were performed. Error bars are the SD of the mean (n = 3).

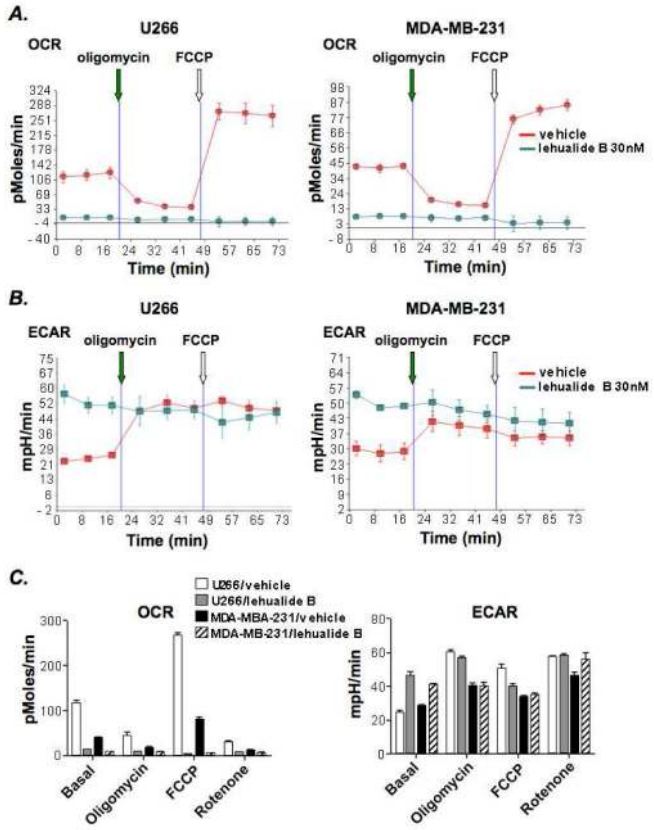

Figure 4.

Lehualide B abolishes OXPHOS in multiple myeloma cells. (***A, B***) U266 (*left panels*) and MDA-MB-231 cells (*right panels*) (in 96 wells) were treated with vehicle (orange line) or with lehualide B (30 nM, teal line) for 1 hr and then assessed for OCR (***A***) or ECAR (***B***) using the Seahorse Bioscience XF96 analyzer.[45] Measurements were determined every 7 min for six replicates and error bars are standard error of the mean. After basal measurements cells were treated with the ATP synthase inhibitor oligomycin (green arrow), which induces increases in glycolysis (*i.e.*, ECAR), followed by treatment with the mitochondrial uncoupling agent FCCP (white arrow), which measures mitochondrial respiratory reserves. Results shown are representative of four independent experiments. Note that lehualide B abolishes OCR and mitochondrial respiratory capacity. (***C***) Summary of OCR (*left*) and ECAR (*right*) analyses of U266 MM and MDA-MB-231 breast cancer cells. Note that the basal rates of OCR are ~3-fold higher in U266 MM cells than in MDAMB-231 cells. Rotenone treatment allows measurement of mitochondrial-independent oxygen consumption, which was minimal in both tumor cell lines. Mean values were calculated before (basal) or after oligomycin, FCCP or rotenone treatment.

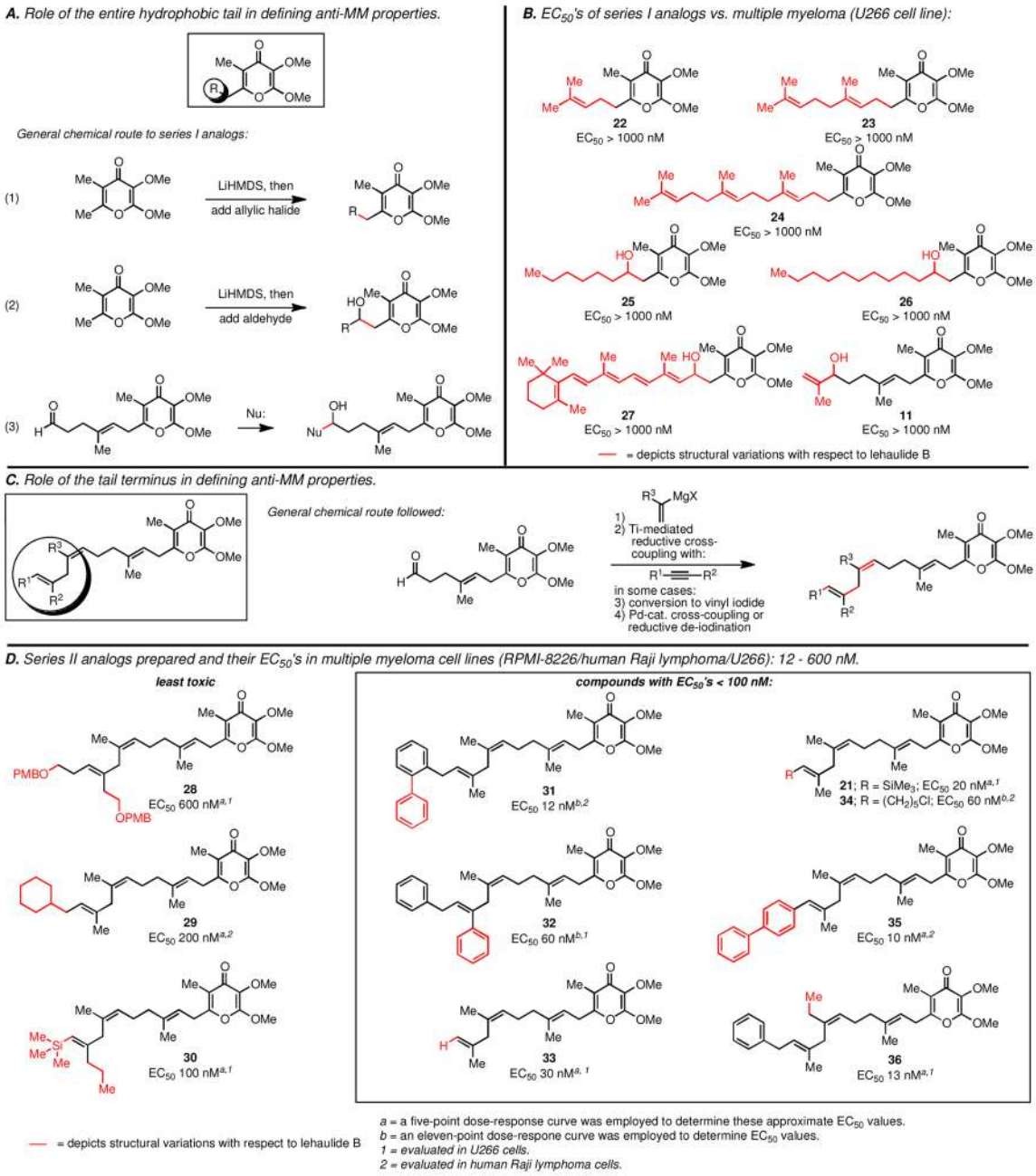

Figure 5.

Synthesis and evaluation of Series I analogs of lehualide B: Significance of the hydrophobic region.

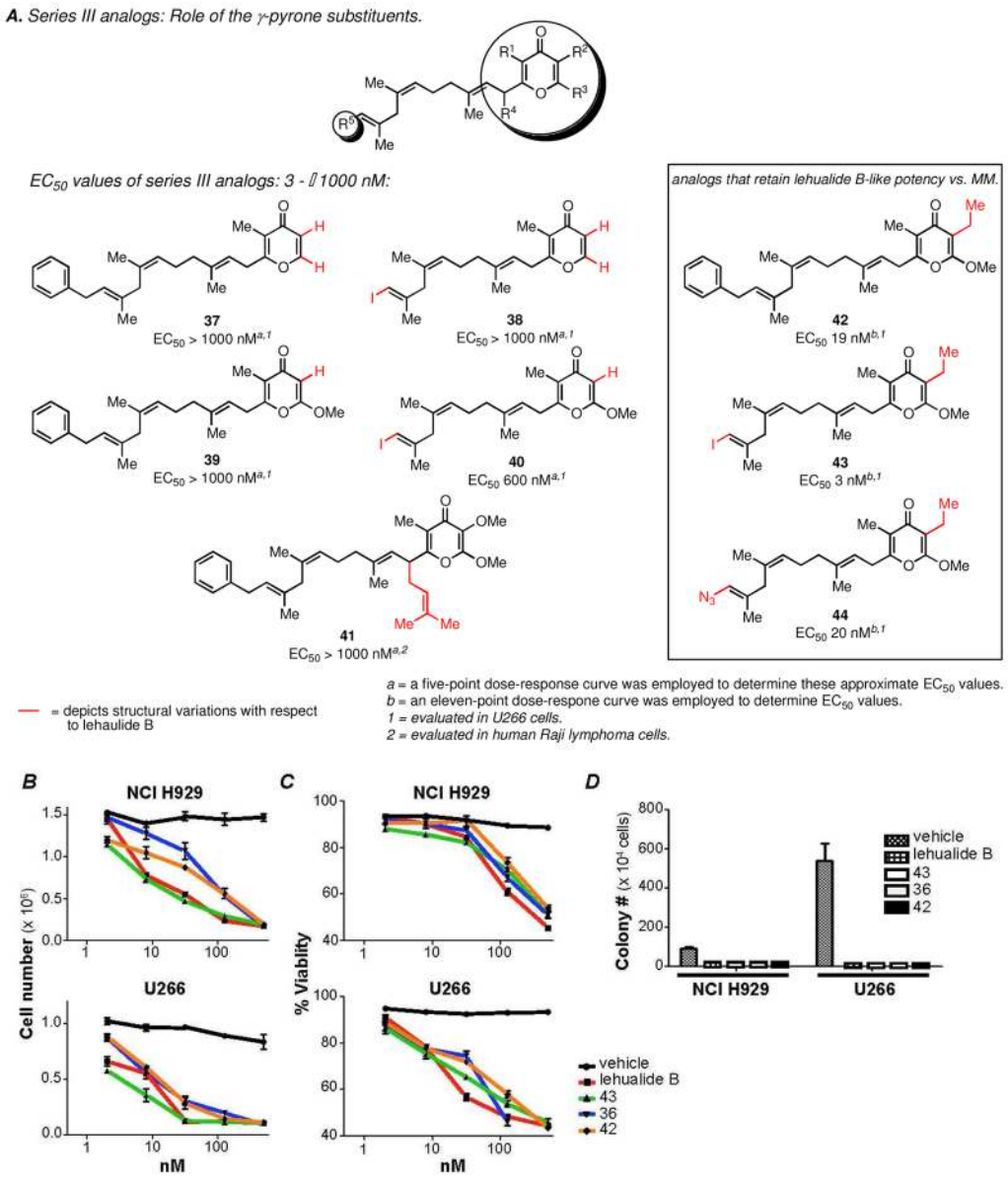

Figure 6.

(***A***) Synthesis and evaluation of Series III analogs of lehualide B: Significance of substitution about the γ-pyrone hydrophilic head. Lehualide B and key analogs compromise growth and survival of multiple myeloma. (***B-C***) NCI H929 and U266 cells were cultured for 3 days with vehicle or the indicated doses of lehualide B or key analogs and cell number (***B***) and percent viable cells (*i.e.*, those excluding trypan blue) (***C***) were determined by counting with a hemocytometer. (***D***) The indicated MM cells were plated in methylcellulose containing the indicated agents (500 nM). Colony numbers were determined on day 10. Error bars are the SD.

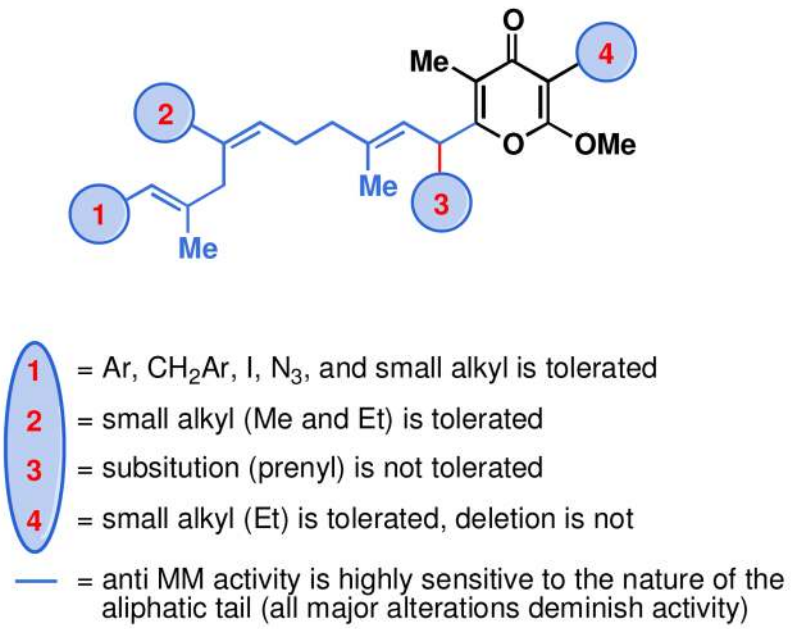

Figure 7.
Summary of lehualide B analogs: SAR for anti-MM activity.

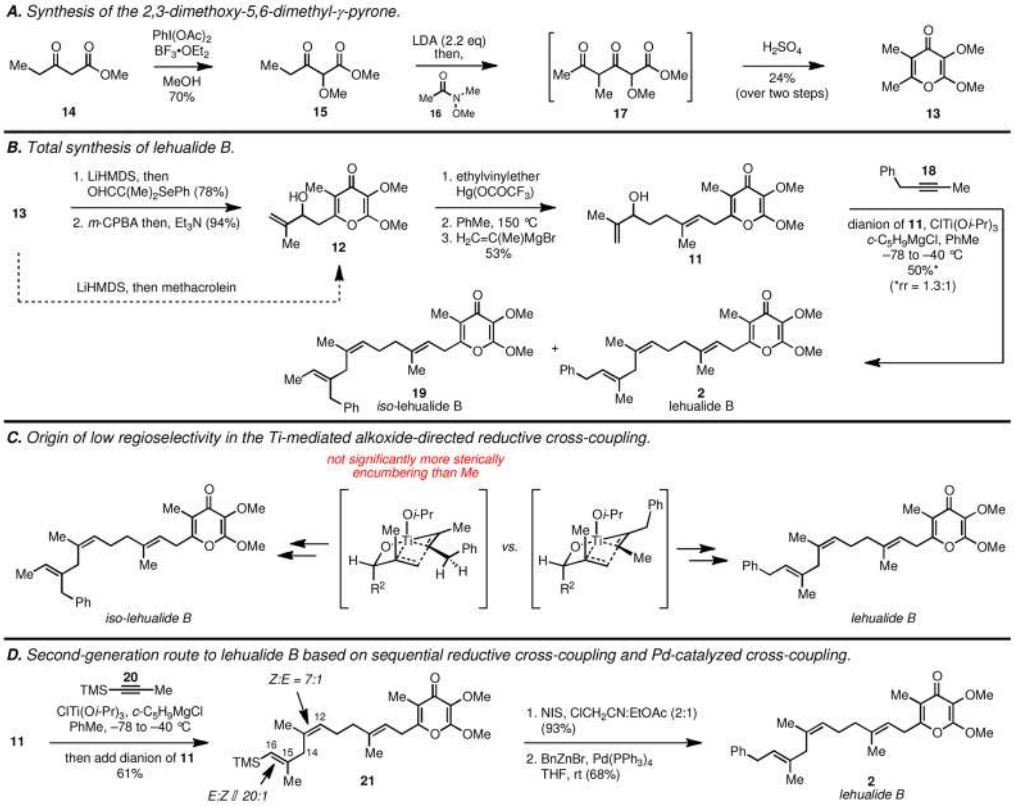

Scheme 1.
Synthesis of lehualide B.